

Separable Representations of Local Potentials

GERHARD W. BUND and HAMIEL A. CONSONI **

Instituto de Física Teórica *, São Paulo SP*

Recebido em 23 de Junho de 1976

The Ernst-Shakin-Thaler (EST) method, which approximates a local potential by one that contains a number of separable terms, by utilizing as basis of expansion a set of states belonging to the discrete and continuous spectra of the Hamiltonian, is discussed and applied to a simple Yukawa potential, and to the Malfliet-Tjon π s potential as Well. We make a comparison between the off-shell R-matrices and phase-shifts corresponding to the local potentials and those obtained from second and third degree EST approximations. A reasonable agreement, particularly with regard to the phase-shifts, was found for energies up to about 150 MeV. The replacement of the state with zero energy by the bound state, in the basis of the EST potential, did not improve the agreement.

O método de Ernst, Shakin e Thaler, (EST) concebido para aproximar um potencial local por outro contendo um dado Número de termos separáveis, e que utiliza, como base de expansão, estados pertencentes aos espectros contínuo e discreto da hamiltoniana, é discutido e aplicado a um potencial de Yukawa, como também ao potencial π s de Malfliet e Tjon. Fazemos uma comparação numérica das matrizes R, fora da camada da energia, e das fases associadas ao potencial local, com as obtidas através da aproximação EST. Para energias até 150 MeV, encontrou-se uma concordância razoável, particularmente com relação às fases. A substituição do estado de energia zero pelo estado ligado, na base de expansão do potencial EST não melhorou a concordância.

* Present address: *Departamento de Física, Universidade Federal de Pernambuco, 50000 - Recife PE.*

** Postal address: *Caixa Postal 5956, 01000-São Paulo SP.*

1. INTRODUCTION

Much effort has been devoted to the description of the nucleon-nucleon interactions through separable potentials¹⁻³. The advantage of having separable potentials is, of course, that the three-body⁴⁻⁶, and also the nuclear matter calculations², become much simpler.

In recent years, several methods have been devised for the construction of separable approximations⁷⁻¹⁰ to local potentials. More explicitly, the aim of these approaches is to obtain potentials, with a few separable terms only, which yield low energy phase-shifts, and off-shell T-matrices, which fit, as closely as possible, those derived from a given local potential.

The best known of these separable approximations is the Unitary Pole Approximation⁸ (UPA), which gives a one term separable potential which takes into account the pole of the T-matrix generated by the bound state of the local potential. A generalization of the UPA is the Unitary Pole Expansion⁸ (UPE) which gives a separable expansion of the local potential, using as a basis the eigenfunctions of the kernel of the Lippmann-Schwinger equation appropriate to that potential.

We shall, in this paper, concern ourselves with the separable potential called EST⁹, which has the property that it generates the same wave functions as the local one, at a number of conveniently chosen energies. The EST method may also be considered a generalization⁹ of the UPA, as the UPA potential generates correctly the bound state of the local potential. However, at the price of having more separable terms, the EST potential is able to reproduce, in addition, a given set of states in the continuum.

The usefulness of any of these methods lies in its ability to yield good approximations. In practice, this means that the low energy T-matrices, derived from a separable potential of second or third degrees, should give a satisfactory fit to those obtained from the local one. Thus, it becomes important to perform numerical tests. In the

case of the EST potential, two such tests have been made, one for a square-well potential¹¹, and the other for a modified Reid¹² potential; both tests have produced good fits.

In the present study, we compare the exact and EST s-wave phase-shifts, and off-shell R-matrices, for a simple Yukawa potential and for the Malfliet-Tjon¹³ 3S_1 potential. We restricted ourselves to separable EST potentials of second and third degrees. In order to obtain the R-matrix corresponding to the local potential, the method of Kowalski-Noyes¹⁴⁻¹⁶ was employed.

In Section 2, a summary of the EST method is given, and in Section 3 we derive expressions for the separable T and R-matrices, and present a brief discussion of the version of the Kowalski-Noyes' method utilized in the present work. Finally, Section 4 is devoted to the presentation and discussion of the results obtained.

2. THE EST POTENTIAL

We shall work in the representation of fixed orbital angular momentum. As our starting potential is central, all relevant matrix elements are diagonal in orbital spin and orbital spin projection. We may thus suppress the angular momentum quantum numbers, and a free two-nucleon state, corresponding to the center of mass energy k^2 ($\hbar = m = 1$), will be denoted simply by $|k\rangle$. The normalization and completeness relations we shall use are

$$\langle k | k' \rangle = \frac{1}{k^2} \delta(k - k'), \quad (1)$$

$$\int |k\rangle \langle k| dk = 1. \quad (2)$$

The separable EST potential, \hat{B} , of degree N, associated to the potential V, is defined by⁹

$$\hat{V} = \sum_{i,j=1}^N V | \psi_i \rangle M_{ij} \langle \psi_j | V, \quad (3)$$

where the hermitian matrix, M is given by

$$\sum_{j=1}^N M_{ij} \langle \psi_j | V | \psi_k \rangle = \sum_{j=1}^N \langle \psi_i | V | \psi_j \rangle M_{jk} = \delta_{ik} . \quad (4)$$

In Eqs. (3) and (4), the states ψ_i are bound-states or states in the continuum, which are solutions of the **Schrodinger** equation corresponding to the potential V . Thus, we write

$$|\psi\rangle = \begin{cases} |\phi(B_i)\rangle, & i = 1, \dots, N_B \\ |\psi(k_{E_i})\rangle, & i = N_B+1, \dots, N \end{cases} \quad (5)$$

where $\phi(B_i)$ represents bound states, $B_i = -E_i$ being the binding energy, and $\psi(k_{E_i})$ the states in the continuum corresponding to the energy $E_i = k_{E_i}^2$.

Here we make the remark that Eqs. (3) and (4) are a common starting point of several methods^{8,10} dealing with the construction of separable approximations to local potentials; these methods are thus distinguished by their prescriptions for the functions ψ_i only.

The normalization of the states ψ_i need not be supplied as it can be easily shown from Eqs. (3) and (4) that the multiplication of ψ_i by an arbitrary constant factor does not alter \hat{V} . This result has the consequence that the asymptotic boundary conditions on the states $\psi(k_{E_i})$ may be arbitrarily chosen. We shall adopt for convenience stationary boundary, that is $\psi(k_{E_i})$ is supposed to satisfy the integral equation

$$|\psi(k_{E_i})\rangle = |k_{E_i}\rangle + G_0^P(E_i) V |\psi(k_{E_i})\rangle, \quad (6)$$

where $G_0^P(E)$ is the principal value Green's function, i.e.,

$$G_0^P(E) = \frac{P}{E - H_0} \quad (7)$$

Here, H is the kinetic-energy operator. The scattering solutions, subject to *outgoing* boundary conditions, shall be denoted by $\psi^+(k_E)$. They satisfy Eq. (6), with $G_0^P(E)$ replaced by $G_0^\pm(E) = (E - H_0 \pm i\epsilon)^{-1}$.

We next present the most relevant properties of the EST potential, \hat{V} . A result which follows from Eqs. (3) and (4), for arbitrarily chosen functions, ψ_i , that is, which is applicable to other methods besides the EST, is the relation

$$V|\psi_i\rangle = \hat{V}|\psi_i\rangle, \quad i = 1, \dots, N. \quad (8)$$

Thus, from Eq. (3), one gets

$$\hat{V}|\psi_i\rangle = \sum_{j,k} V|\psi_j\rangle M_{jk} \langle \psi_k | V | \psi_i \rangle. \quad (9)$$

The application of Eq. (4), to the right hand side of Eq. (9), yields Eq. (8).

In the case of the EST potential, one gets, in addition, that the state $\psi(k_{E_i})$, defined by Eq. (6), coincides with the corresponding state $\hat{\psi}(k_{E_i})$, appropriate to the potential \hat{V} , which satisfies the equation

$$|\hat{\psi}(k_{E_i})\rangle = |k_{E_i}\rangle + G_0^P(E_i) \hat{V}|\hat{\psi}(k_{E_i})\rangle. \quad (10)$$

That is, for the EST potential one has the relationship

$$|\psi(k_{E_i})\rangle = |\hat{\psi}(k_{E_i})\rangle, \quad i = N_B + 1, \dots, N. \quad (11)$$

The above property follows by noting that, if one replaces $V|\psi(k_{E_i})\rangle$, in Eq. (6), by $\hat{V}|\psi(k_{E_i})\rangle$, according to Eq. (8), one finds that $\hat{\psi}(k_{E_i})$ also satisfies Eq. (10).

Furthermore, from the equation for the bound-states in the potential V

$$|\phi(B_i)\rangle = G_0(-B_i) V |\phi(B_i)\rangle, \quad (12)$$

one gets from Eq. (8) that $\phi(B_i)$ is also a bound-state appropriate to the EST potential, with the same binding energy, B_i .

Summarizing the above results, one finds then that both Hamiltonians, $H + V$ and $H_0 + \hat{V}$, have the same eigenstates at the N specified values E_i of the energy spectrum. It can be shown¹⁷ that, if the starting potential, V , is already separable, of degree N , then the EST potential of the same degree coincides with V .

As was pointed out before, we may replace in Eq. (5), $\psi(k_i)$ by $\psi^+(k_{E_i})$, without changing the potential \hat{V} . If one makes this substitution, and follows the steps utilized in derivation of Eqs. (8) and (11), one gets the analogous results

$$V|\psi^+(k_{E_i})\rangle = \hat{V}|\psi^+(k_{E_i})\rangle, \quad i = N_B+1, \dots, N, \quad (13)$$

$$|\psi^+(k_{E_i})\rangle = |\hat{\psi}^+(k_{E_i})\rangle, \quad i = N_B+1, \dots, N. \quad (14)$$

As the half-shell T-matrix satisfies the relation

$$\langle k|T(E)|k_E\rangle = \langle k|V|\psi^+(k_E)\rangle, \quad (15)$$

the results (13) and (14) are equivalent to the statement⁹ that the half-shell T-matrices, $\langle k|T(E_i)|k_{E_i}\rangle$ and $\langle k|\hat{T}(E_i)|k_{E_i}\rangle$, corresponding respectively to potentials V and \hat{V} , do coincide. A similar result, for the half-shell R-matrices, is derived from the relation

$$\langle k|R(E)|k_E\rangle = \langle k|V|\psi(k_E)\rangle. \quad (16)$$

3. THE SEPARABLE AND THE EXACT R-MATRICES

The equation for the T -matrix, which corresponds to the separable potential \hat{V} , i.e.,

$$\hat{T}(E) = \hat{V} + \hat{V}G_0^+(E)\hat{T}(E), \quad (17)$$

is easily solved. According to Eqs. (3) and (17), \hat{T} must be of the form

$$\hat{T}(E) = \sum_{i,j} V|\psi_i\rangle t_{ij}(E)\langle\psi_j|V. \quad (18)$$

Inserting the expression (18) into Eq. (17), one gets, after some manipulations¹⁷, the equation

$$\sum_j t_{ij}(E)\langle\psi_j|(V - VG_0^+(E)V)|\psi_k\rangle = \delta_{ik}. \quad (19)$$

which determines the matrix $t(E)$.

Instead of comparing the exact and EST T -matrices, we shall do so for the R -matrices. We found it more convenient to work with the R -matrix, as the latter is a real symmetric matrix for real potentials. Once the R -matrix is determined, the T -matrix may easily be obtained from the Heitler relation^{18,19}:

$$\begin{aligned} \langle k|T(E)|k'\rangle &= \langle k|R(E)|k'\rangle \\ &- i\pi k_E \frac{\langle k|R(E)|k_E\rangle\langle k_E|R(E)|k'\rangle}{2 + i\pi k_E\langle k_E|R(E)|k_E\rangle}. \end{aligned} \quad (20)$$

This approach has the additional advantage that the unitarity of the T -matrix, which follows from the hermiticity of the R -matrix, is preserved.

The equation for the separable R -matrix, $\hat{R}(E)$, is obtained from Eq. (17) by replacing $G_0^+(E)$ by $G_0^P(E)$. By following the steps used in the derivation of⁹, one obtains the result, analogous to Eqs. (18) and (19),

$$\hat{R}(E) = \sum_{i,j} V|\psi_i\rangle r_{ij}(E) \langle\psi_j|V, \quad (21)$$

where the N-dimensional matrix, $r(E)$, is given by

$$(r^{-1})_{ij} = \langle\psi_i|V|\psi_j\rangle - \langle\psi_i|VG_0^P(E)V|\psi_j\rangle. \quad (22)$$

Either by applying the Heitler relation, Eq. (20), or by replacing $G_0^+(E)$, in Eq. (19), by $G_0^P(E) - i\pi\delta(E-H_0)$, one derives** the following expression:

$$t_{ij}(E) = r_{ij}(E) - \frac{i\pi k_E (\sum_n r_{in} \langle\psi_n|V|k_E\rangle) (\sum_m \langle k_E|V|\psi_m\rangle r_{mj})}{2 + i\pi k_E \sum_{m,n} \langle k_E|V|\psi_m\rangle r_{mn} \langle\psi_n|V|k_E\rangle}, \quad (23)$$

which gives $t_{ij}(E)$ directly in terms of the $r_{ij}(E)$.

The separable potential, and the corresponding R and T-matrices, may be expressed exclusively in terms of the matrix elements $\langle k|V|\psi_i\rangle$, which coincide with the half-shell R-matrices (cf. Eq. (16)) for ψ_i belonging to the continuous spectrum of $H_0 + V$. Thus, the matrix element $\langle\psi_i|V|\psi_j\rangle$, which appears in Eqs. (4) and (22), may be written

$$\begin{aligned} \langle\psi_i|V|\psi_j\rangle = \eta_i \langle k_{E_i}|V|\psi_j\rangle + \int_0^\infty \frac{dk}{E_i - k^2} \{ k^2 \langle\psi_i|V|k\rangle \langle k|V|\psi_j\rangle \\ - \eta_i k_{E_i}^2 \langle\psi_i|V|k_{E_i}\rangle \langle k_{E_i}|V|\psi_j\rangle \}, \end{aligned} \quad (24)$$

where $\eta_i=0$, if the state ψ_i is a bound state, and $\eta_i=1$, if it belongs to the continuum. The expression (24) was obtained by replacing in the matrix element, $\langle\psi_i|V|\psi_j\rangle$, ψ_i by the right hand side of Eqs. (6) or (12), in the cases $\eta_i=0$ and $\eta_i=1$, respectively.

The second term, on the right hand side of Eq. (22), may be written more explicitly as

$$\begin{aligned} \langle \psi_i | V G_0^P(E) V | \psi_j \rangle = & \int_0^\infty \frac{dk}{E - k^2} \{ k^2 \langle \psi_i | V | k \rangle \langle k | V | \psi_j \rangle \\ & - k_E^2 \langle \psi_i | V | k_E \rangle \langle k_E | V | \psi_j \rangle \} . \end{aligned} \quad (25)$$

The evaluation of the principal value integrals, leading to Eqs. (24) and (25), was accomplished by making use of the relation

$$\int_0^\infty \frac{P}{E - k^2} f(k) dk = \int_0^\infty \frac{f(k) - f(k_E)}{E - k^2} dk . \quad (26)$$

The R -matrix appropriate to the local potential, V , is given by the integral equation

$$R(k, k', E) = V(k, k') + \int_0^\infty V(k, q) \frac{P}{E - q^2} q^2 R(q, k', E) dq , \quad (27)$$

where we introduced the notation

$$V(k, k') = \langle k | V | k' \rangle , \quad (28)$$

$$R(k, k', E) = \langle k | R(E) | k' \rangle . \quad (29)$$

In order to avoid the singularity of the kernel, at $q=k_E$, which makes the direct numerical integration of Eq.(27) difficult, we employed the Kowalski-Noyes method, which achieves the reduction of Eq.(27) to an integral equation with a nonsingular kernel, in addition to a quadrature which determines the on-shell R -matrix.

According to the version of the Kowalski-Noyes procedure we have adopted, one solves first the integral equation

$$B(k, k', E) = V(k, k') + \int_0^\infty \Lambda(k, q, E) B(q, k', E) dq, \quad (30)$$

where the kernel,

$$\Lambda(k, k', E) = \left[V(k, k') - \frac{V(k, k_E) V(k_E, k')}{V(k_E, k_E)} \right] \frac{k'^2}{E - k'^2}, \quad (31)$$

is nonsingular. In terms of the B-matrix, the R-matrix reads

$$R(k, k', E) = B(k, k', E) - B(k, k_E, E) V_E^{-1} V(k', k_E) + \\ B(k, k_E, E) R_E V_E^{-2} B(k', k_E, E), \quad (32)$$

where V_E and R_E denote respectively the matrix elements $V(k_E, k_E)$, and $R(k_E, k_E, E)$, the latter being given by

$$R_E = V_E^2 \left\{ V_E - \int_0^\infty \frac{dk}{E - k^2} \left[k^2 V(k_E, k) B(k, k_E, E) - k_E^2 V_E^2 \right] \right\}^{-1}. \quad (33)$$

We remark here that the integrand, in Eq.(31), has no singularity at $k = k_E$, by virtue of the relation

$$B(k_E, k, E) = V(k_E, k), \quad (34)$$

which follows from Eqs. (30) and (31). For the half-shell R-matrix, which is the only input required for the evaluation of the separable R-matrix, one gets from Eqs. (32) and (34)

$$\langle k | R(E) | k_E \rangle = B(k, k_E, E) R_E V_E^{-1}. \quad (35)$$

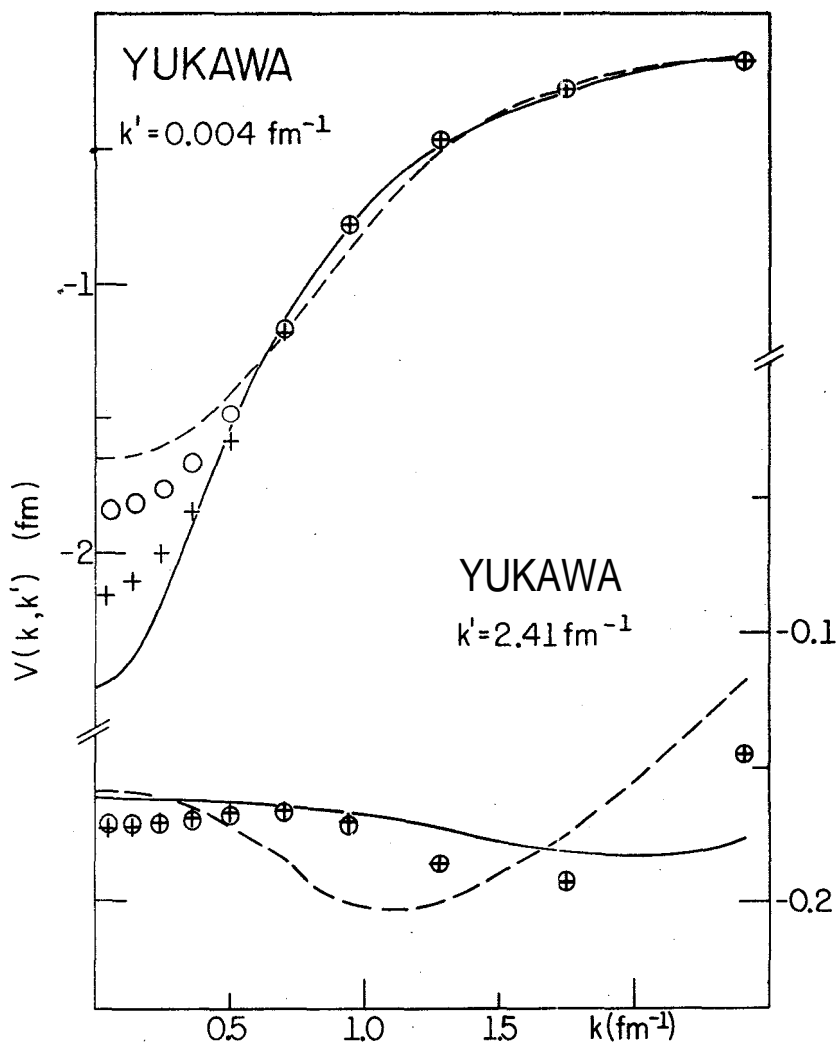


Fig. 1 - Matrix elements, $V(k, k')$, for the exact and approximate Yukawa potential as function of k , for $k' = 0.004 \text{ fm}^{-1}$, and 2.41 fm^{-1} . The full line corresponds to the local potential Y ; the broken line to the EST potential $Y1$, with expansion energies 0.061 MeV, and 52.37 MeV; the circles to the potential $Y2$, with expansion energies 0.061 MeV, 28.29 MeV, and 97.17 MeV; the crosses to potential $Y3$, with expansion energies -2.25 MeV, 28.29 MeV, and 97.17 MeV.

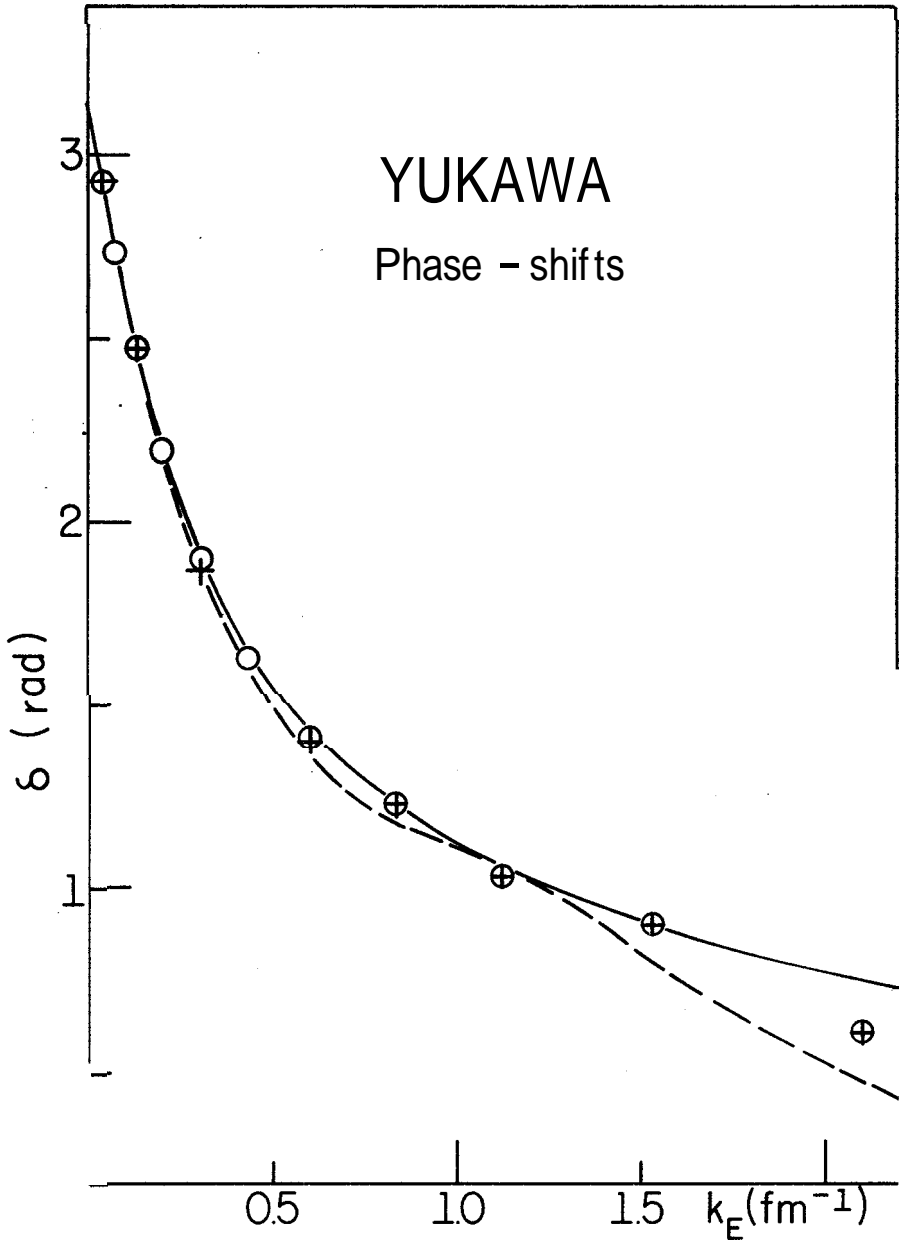


Fig. 2 - Phase shifts, $\delta(k_E)$, versus k_E ($k_E^2 = E$, $1\text{fm}^{-2} = 41.5 \text{ MeV}$), for the Yukawa potential Y (full line); the EST potential Y1 (broken line); the potential Y2 (circles), and the potential Y3 (crosses).

4. NUMERICAL APPLICATIONS OF THE EST METHOD

We performed a numerical test of the EST method for a simple Yukawa potential, and for the Malfliet-Tjon¹³ 3S_1 potential III, the latter consisting in the superposition of two Yukawa potentials.

Let us first describe the results for the Yukawa potential

$$V_Y(r) = A \frac{e^{-ar}}{r}, \quad (36)$$

for which the following assignment was made¹⁰:

(Y) $A = -65.25 \text{ MeVfm}$, $a = 0.632 \text{ fm}^{-1}$. This potential has a bound-state at -2.245 MeV ($1 = \hbar^2/m = 41.5 \text{ MeV fm}^2$).

We studied the following choices for the expansion energies: E_i , $i = 1, \dots, N$, which define the set of states ψ_i utilized as a basis in the construction of the EST potential (cf. Eq. (5)):

(Y1) $N = 2$, $E_1 = 0.061 \text{ MeV}$, $E_2 = 52.370 \text{ MeV}$;

(Y2) $N = 3$, $E_1 = 0.061 \text{ MeV}$, $E_2 = 28.286 \text{ MeV}$, $E_3 = 97.172 \text{ MeV}$;

(Y3) $N = 3$, $E_1 = -2.245 \text{ MeV}$, $E_2 = 28.286 \text{ MeV}$, $E_3 = 97.172 \text{ MeV}$.

The only difference between the potentials Y2 and Y3 is that, for the state corresponding to the lowest expansion energy, we used the bound-state in Y3. The purpose for considering this last case was to test whether the replacement of a state, with a slightly positive energy, by the bound state would improve the fit, as one would expect from the fact that potential Y3 is an extension of the UPA potential.

In Fig. 1, we plot the matrix elements $\langle k|V|k' \rangle$, for the local potential, Y together with those for the separable ones, Y1, Y2 and Y3 as function of k , for $k' = 0.004 \text{ fm}^{-1}$, and $k' = 2.407 \text{ fm}^{-1}$. In Fig. 2, a comparison between the exact phase shifts, plotted as function of k_E ,

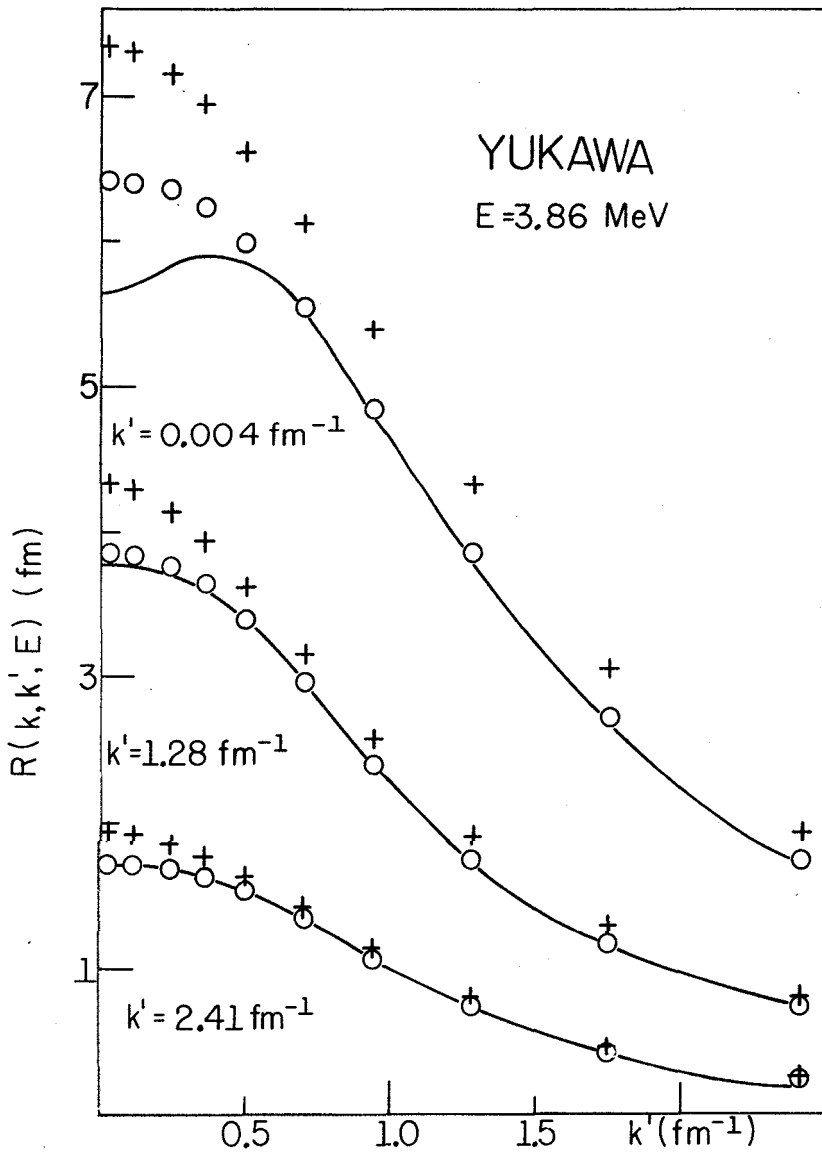


Fig.3a - Off-shell R -matrix elements, $R(k, k', E)$, as function of k , for $k' = 0.004 \text{ fm}^{-1}$, 1.28 fm^{-1} , 2.41 fm^{-1} , and $E = 3.86 \text{ MeV}$ ($k_E = 0.305 \text{ fm}^{-1}$). The full line corresponds to the Yukawa potential; the EST potentials Y2 and Y3 are represented respectively by circles and crosses.

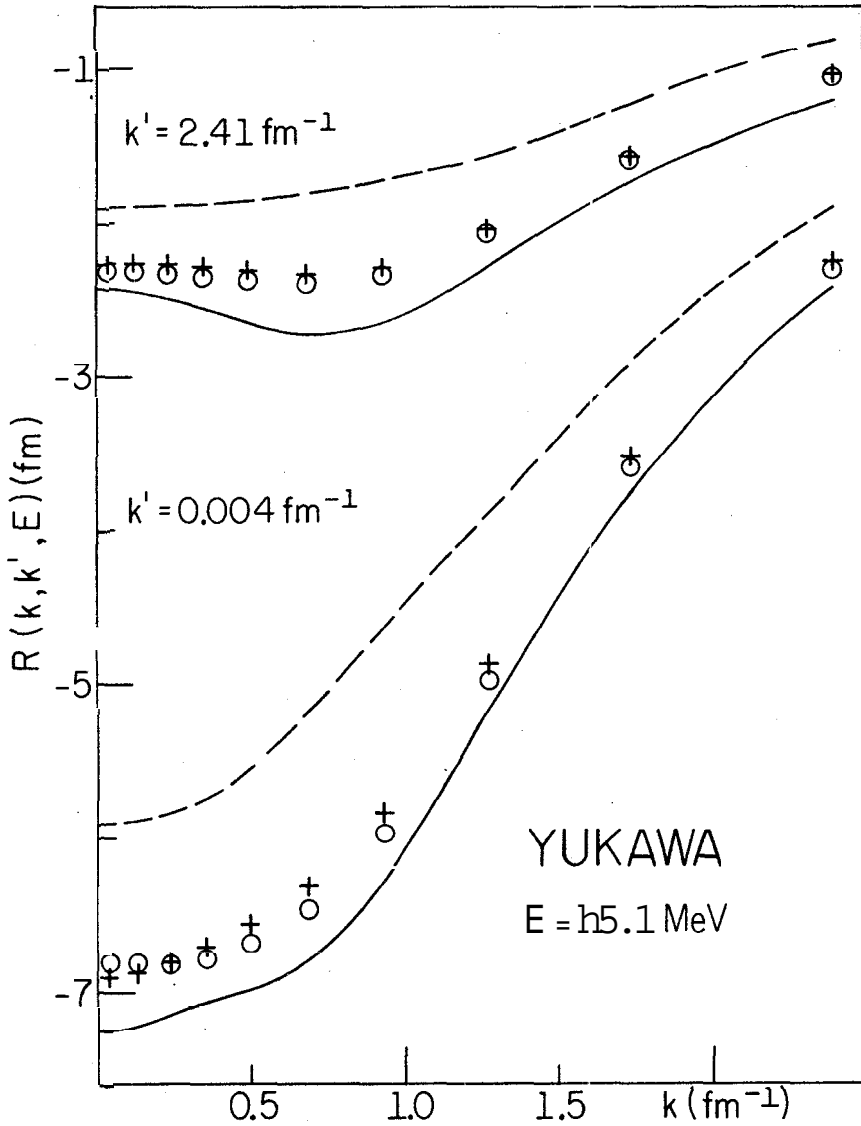


Fig.3b - Off-shell R-matrix elements, $R(k, k', E)$, as function of k , for $k' = 0.004 \text{ fm}^{-1}$, and 2.41 fm^{-1} , and $E = 15.09 \text{ MeV}$ ($k_E = 0.603 \text{ fm}^{-1}$). The full line corresponds to the Yukawa potential. The EST cases Y1, Y2, and Y3, are represented respectively by a broken line, circles and crosses.

and those corresponding to the separable potentials, is made. For values of k_E , up to about 1.5 fm^{-1} ($E = 91 \text{ MeV}$), one finds a better than 10 percent agreement in the case Y1. In cases Y2 and Y3, the largest discrepancy, between the EST and exact phase-shifts, is less than 3 percent in the above range of values of k_E .

In Fig. 3a, we present the exact and the separable R-matrices, $\langle k | R(E) | k' \rangle$, as function of k , at one small, one large and one intermediate value of k' , for $E = 3.86 \text{ MeV}$. In Fig. 3b, similar results for $E = 15.09 \text{ MeV}$ are given. In Fig. 3a, we omitted the results corresponding to the potential Y1, which were found to lie very close to those for the potential Y2, as they would obscure the figure.

One sees, from Fig. 3a, that the substitution of a state with positive energy by the bound state, in the basis of the EST potential, does not necessarily lead to an improvement of the fit. In Fig. 3b, the points corresponding to potentials Y2 and Y3 are very close, while at still higher energies they were found to overlap practically. This last result is expected, since E is now large compared to the binding energy.

We next discuss our results for the Malfliet-Tjon potential:

$$V_M(r) = A \frac{e^{-ar}}{r} + B \frac{e^{-br}}{r}, \quad (37)$$

where the parameters have the values¹³:

$$\begin{aligned} (M) \quad A &= -627.23 \text{ MeV fm}, \quad a = 1.55 \text{ fm}^{-1}, \\ B &= 1439.5 \text{ MeV fm}, \quad b = 3.11 \text{ fm}^{-1}. \end{aligned}$$

This potential has a bound state at -2.230 MeV , appropriate to the deuteron.

We give here results for the following choices of EST potentials:

$$(M1) \quad N = 2, \quad E_1 = 15.440 \text{ MeV}, \quad E = 113.144 \text{ MeV};$$

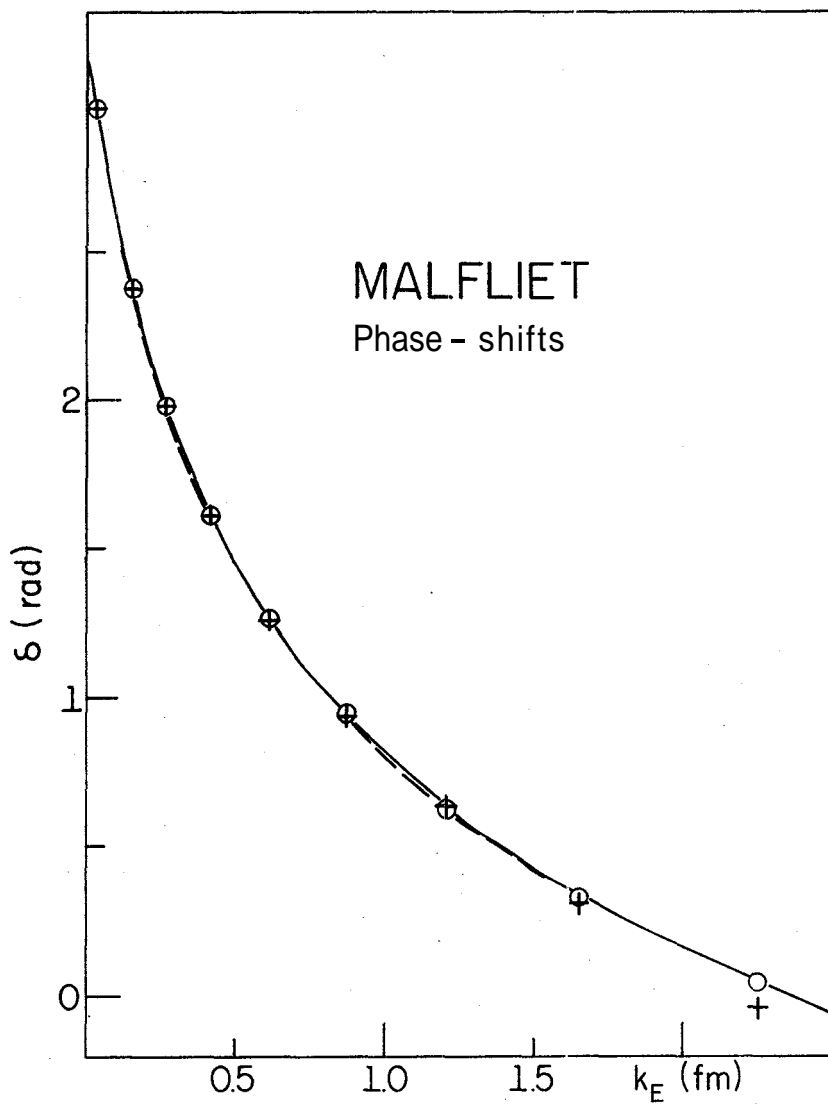


Fig. 4 - Phase shift, $\delta(k_E)$, versus k_E , for the Malfliet-Tjon potential M (full line); the EST potential M1, with expansion energies 15.44 MeV and 113.1 MeV (broken line); the potential M2, with expansion energies 0.035 MeV, 31.27 MeV and 209.5 MeV (circles); potential M3, with expansion energies 0.035 MeV, 60.34 MeV, and 388.7 MeV (crosses).

(M2) $N = 3$, $E_1 = 0.035$ MeV, $E_2 = 31.267$ MeV, $E_3 = 209.481$ MeV;

(M3) $N = 3$, $E_1 = 0.035$ MeV, $E_2 = 60.344$ MeV, $E_3 = 388.690$ MeV.

In Fig.4, the comparison of the phase shifts is presented. The agreement between the EST and the exact phase-shifts is almost perfect, for k_E up to 2.0 fm^{-1} ($E = 162$ MeV), for the potentials M1 and M2. In Figs. 5a - 5i, the separable and exact R-matrix elements are presented as function of k , for three values of k' , and three values of E . In the region of very large values, of both k and k' (cf. Fig.5e), the exact and separable R-matrices differ often by a factor of five or more. This large ratio is compensated by the fact that, in this region these matrix elements become very small in magnitude, and are thus expected to yield negligible contributions to the three-body calculations.

Like in the case of the Yukawa potential, we also performed, for the Malfliet-Tjon potential, calculations using an EST potential M4, which is obtained from the case M3 by making the replacement of the state corresponding to the lowest expansion energy, E_1 , by the correct bound state. The results were similar to those obtained for the Yukawa potential, that is, for the lower energies the results were not as good as those of the case M3, whereas, for the higher values of L , the R-matrices corresponding to potentials M3 and M4 are almost identical. We did not make calculations for negative energies, for which the case M4 should yield better results than those for M3.

Here we make the remark that, for both local potentials considered, the phase shifts which correspond to the EST potentials were found never to exceed the exact ones. The phase shifts corresponding to the local potential thus seem to represent an upper limit in the EST method.

We mention here that no effort was made to obtain best fits for the off-shell R-matrices, or phase shifts, by making systematic variations of the expansion energies.

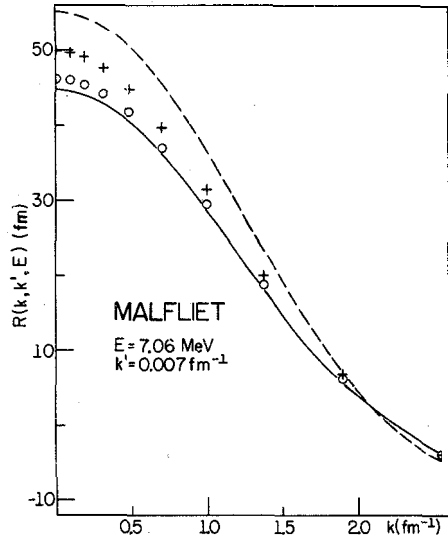


Fig.5a - R-matrix elements, $R(k, k', E)$, as function of k , for $k' = 0.007 \text{ fm}^{-1}$ and $E = 7.06 \text{ MeV}$ ($k_E = 0.412 \text{ fm}^{-1}$). The full line corresponds to the Malfliet potential M; the EST potentials M1, M2 and M3, are represented respectively by a broken line, circles and crosses.

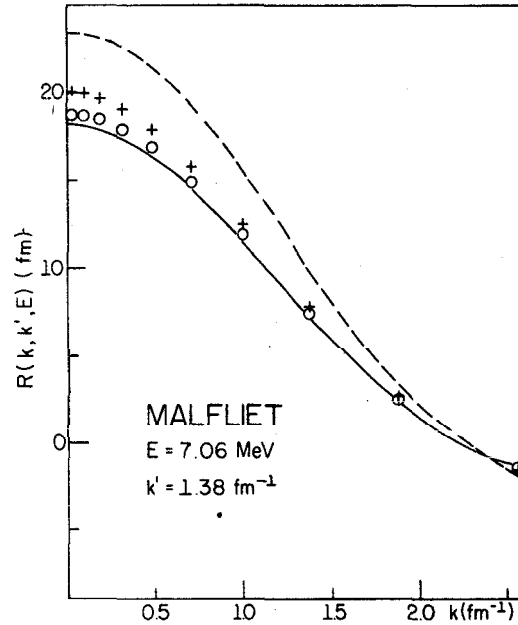


Fig.5b - Same as Fig.5a, for $k' = 1.38 \text{ fm}^{-1}$, end $E = 7.06 \text{ MeV}$ ($k_E = 0.412 \text{ fm}^{-1}$).

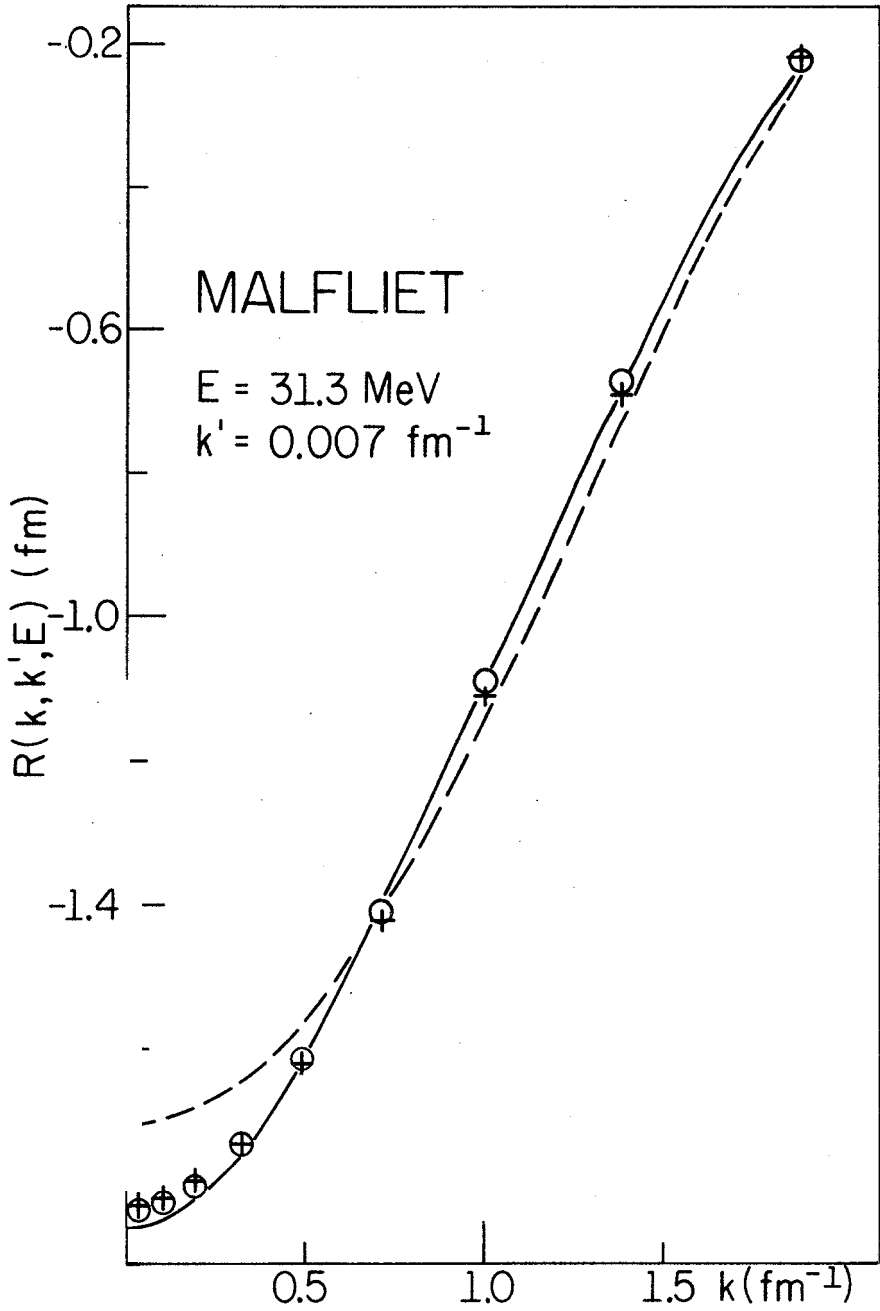


Fig.5c - Same as Fig.5a, for $k' = 0.007 \text{ fm}^{-1}$, and $E = 31.3 \text{ MeV}$ ($k_E = 0.868 \text{ fm}^{-1}$).

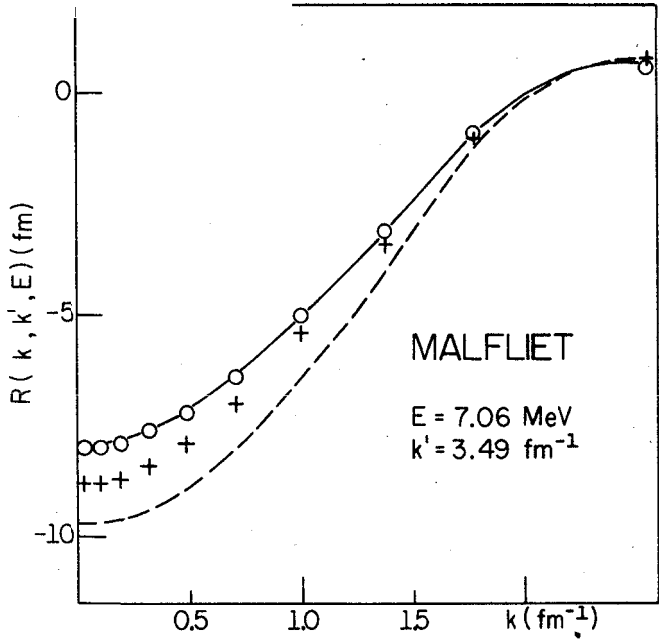


Fig.5d - Same as Fig.5a, for $k' = 3.49 \text{ fm}^{-1}$, and $E = 7.06 \text{ MeV}$ ($k_E = 0.412 \text{ fm}^{-1}$).

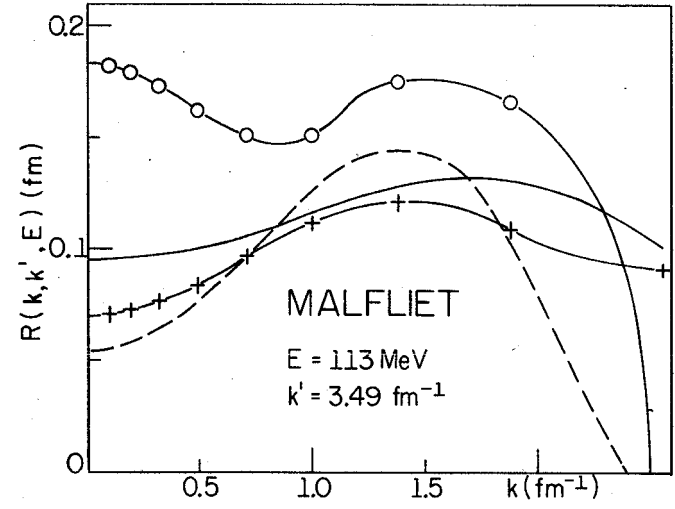


Fig.5e - Same as Fig.5a, for $k' = 3.49 \text{ fm}^{-1}$, and $E = 113 \text{ MeV}$ ($k_E = 1.65 \text{ fm}^{-1}$).

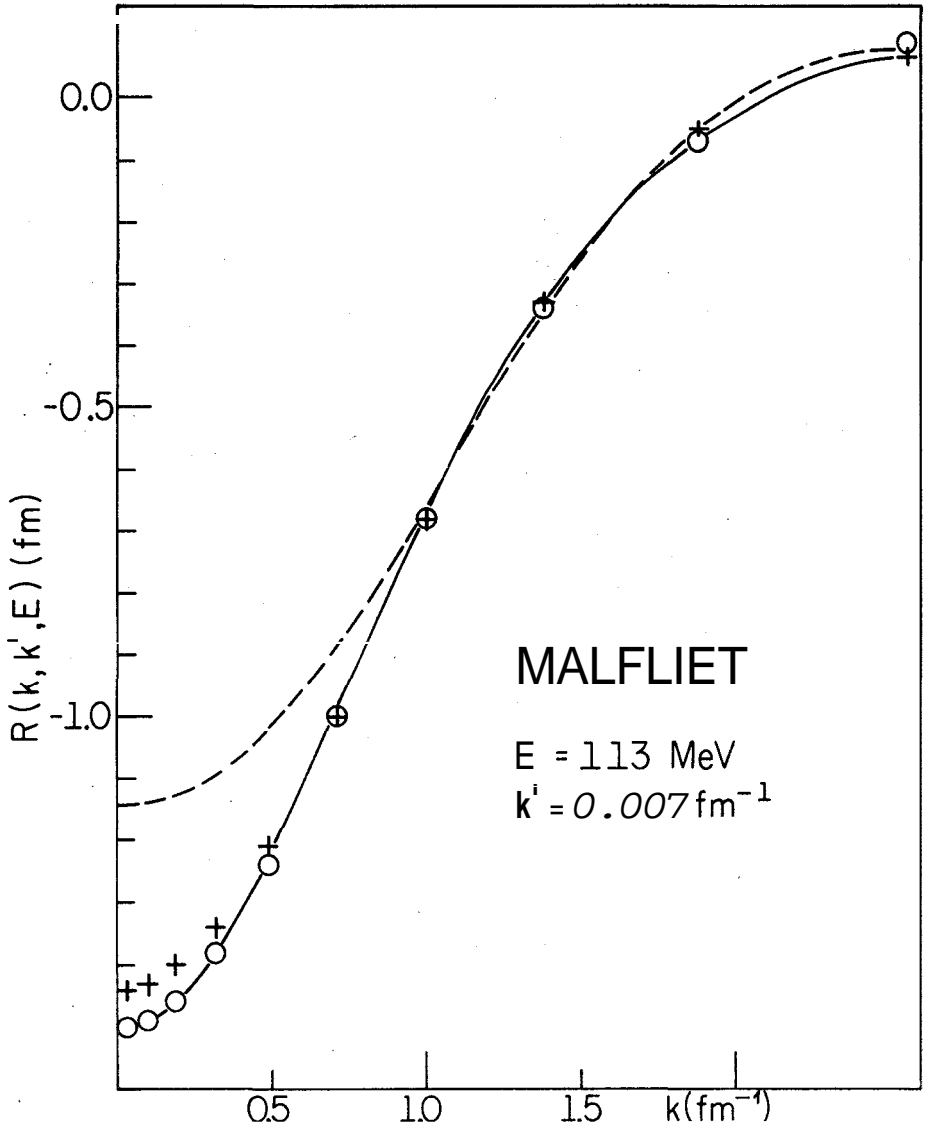


Fig. 5f - Same as Fig. 5a, for $k' = 0.007 \text{ fm}^{-1}$, and $E = 113 \text{ MeV}$ ($k_E = 1.65 \text{ fm}^{-1}$).

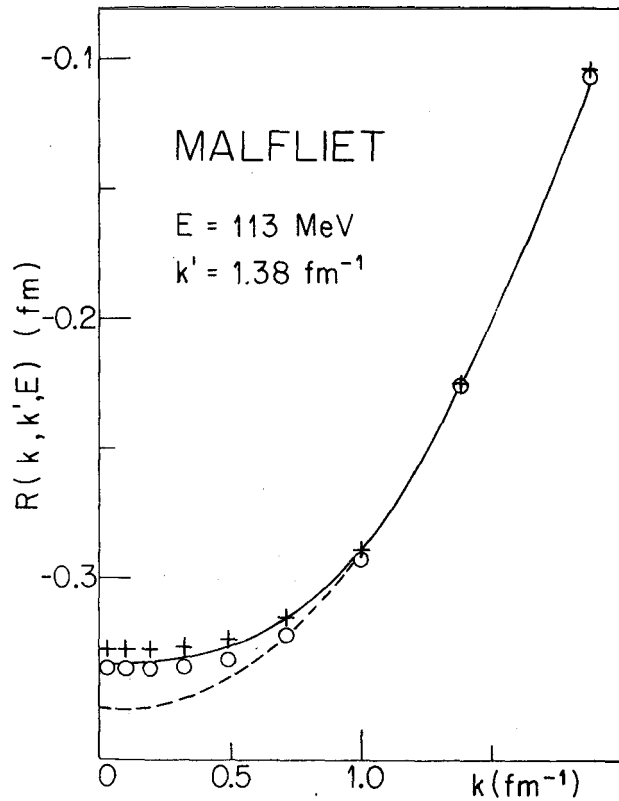


Fig.5g - Same as Fig.5a, for $k' = 1.38 \text{ fm}^{-1}$, and $E = 113 \text{ MeV}$ ($k_E = 1.65 \text{ fm}^{-1}$).

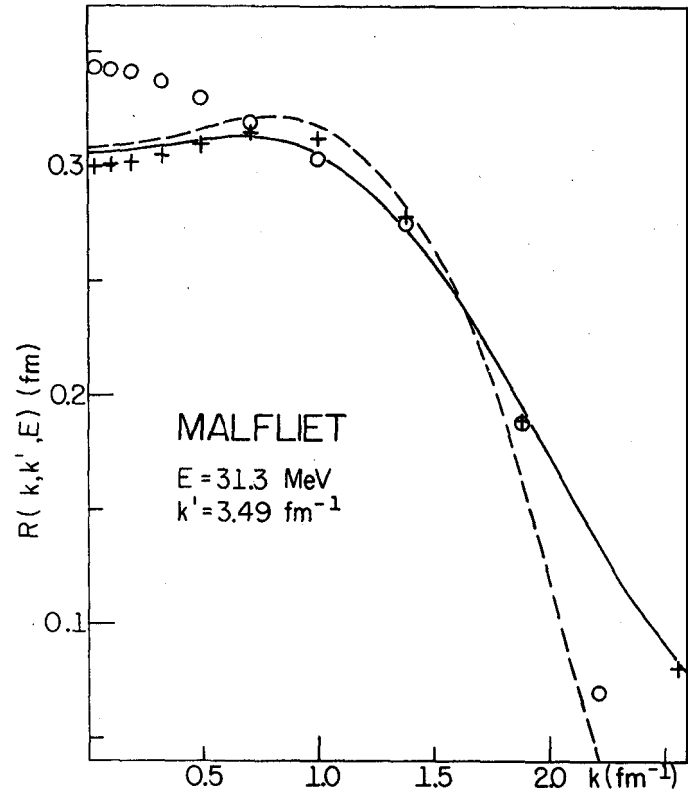


Fig.5h - Same as Fig.5a, for $k' = 3.49 \text{ fm}^{-1}$, and $E = 31.3 \text{ MeV}$ ($k_E = 0.868 \text{ fm}^{-1}$).

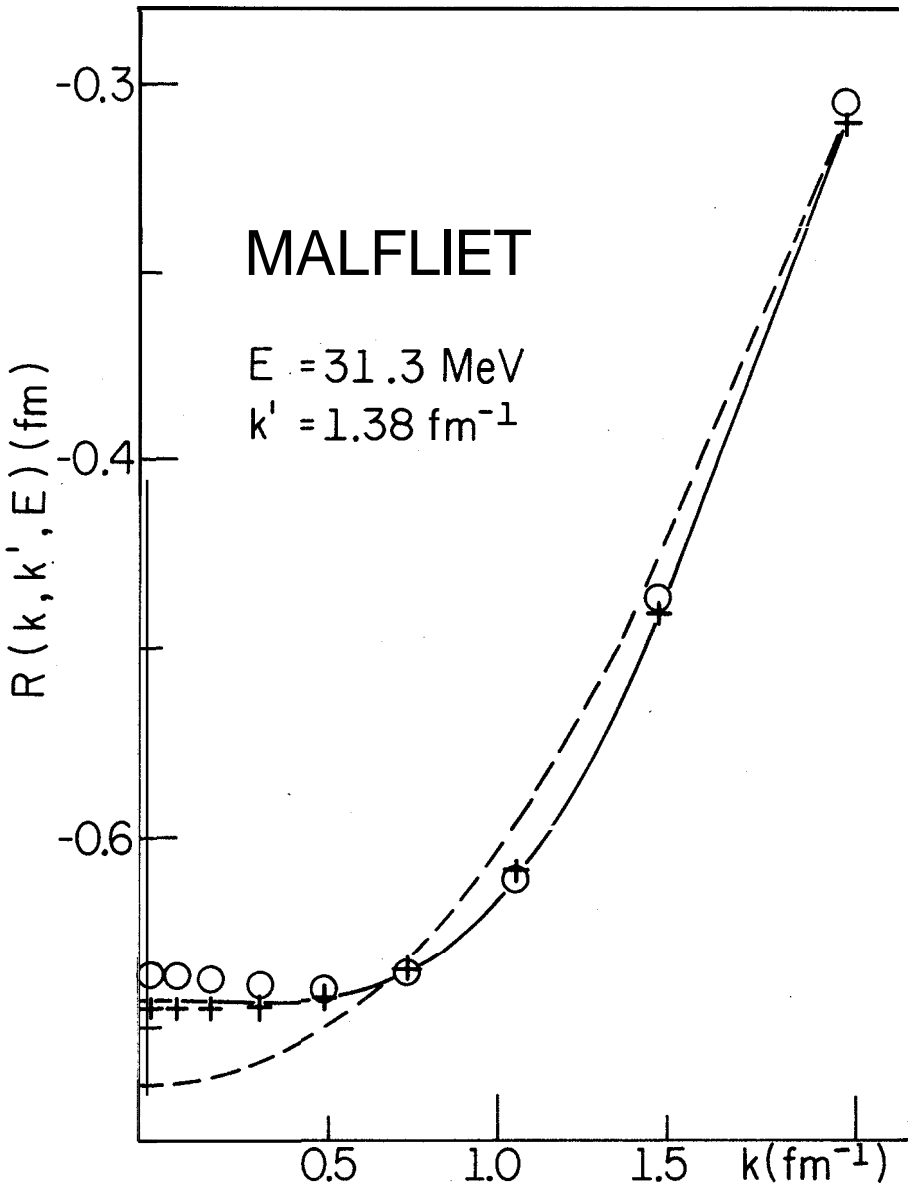


Fig.5i - Same as Fig.5a, for $k' = 1.38 \text{ fm}^{-1}$, and $E = 31.3 \text{ MeV}$ ($k_E = 0.868 \text{ fm}^{-1}$).

The equations used to obtain a numerical solution, for the exact R -matrix were Eqs. (30), (32) and (33). For the separable R -matrix, we utilized Eqs. (21) and (22), coupled to Eqs. (24), (25) and (35).

For the calculations, a 20 points Gaussian mesh, in momentum space, was used. Thus, by approximating the integral, in Eq.(30), by a Gaussian quadrature, the integral equation corresponding to the exact R -matrix is replaced by a system of linear equations, which was solved by means of the Gaussian reduction²⁰. The integrals which appear in Eqs. (24), (25) and (33) were also evaluated through Gaussian quadratures.

The wave functions of the bound state, needed for the calculation of the EST potentials Y_3 and M_4 , were obtained by solving the Schrödinger eigenvalue problem in configuration space. The matrix elements, $\langle k|V|\phi(B_1)\rangle$, where $\phi(B_1)$ is the wave function of the bound state, were evaluated by making Bessel transforms.

A partial check of our computer program was achieved simply by using as input, instead of the local potential, a separable potential of second degree.

REFERENCES

1. Y. Yamaguchi and Y. Yamaguchi, Phys. Rev. 95(1954)1635.
2. F. Tabakin, Ann. of Phys. 30(1964)51.
3. S. Kahana, H.C. Lee and C.K. Scott, Phys. Rev. 185(1969)1378.
4. A.C. Phillips, Nucl. Phys. A107(1968)209.
5. R.T. Cahill and I.H. Sloan, Phys.Lett. 31B(1970)353.
6. R.T. Cahill and I.H. Sloan, Nucl. Phys. A165(1971)161.
7. S. Weinberg, Phys. Rev. 130(1963)776.
8. E. Harms, Phys.Rev. C1(1970)1667.
9. D.J. Ernst, C.M. Shakin and R.M. Thaler, Phys.Rev. C8(1973)46.
10. K. Adhikari, Phys. Rev. C10(1974)1623.
11. D.J. Ernst, C.M. Shakin, R.M. Thaler and D.L. Weiss, Phys. Rev. C8(1973)2056.

12. S.C. Pieper, *Phys.Rev.* C9(1974)883.
13. R.A. Malfliet and J.A. Tjon, *Nucl.Phys.* A127(1969)161.
14. K.L. Kowalski and D. Feldman, *J. Math.Phys.* 4(1963)507.
15. K.L. Kowalski, *Phys. Rev. Lett.* 15(1965)798.
16. H.P. Noyes, *Phys. Rev. Lett.* 15(1965)538.
17. L.H.A. Consoni, *Master Thesis*, Instituto de Física Teórica (1975) unpublished.
18. K.M. Nutall and J. Watson, *Topics in Several Particle Dynamics* (Holden-Day, Inc., San Francisco, 1967) p.19.
19. M.L. Goldberger and K.M. Watson, *Collision Theory* (John Wiley & Sons, Inc., New York, 1964) p.215.
20. F.B. Hildebrand, *Introduction to Numerical Analysis* (McGraw - Hill Book Company, New York, 1956) p.428.